Scharnagl, N.; Hiebl, B.; Trescher, K.; Zierke, M.; Behl, M.; Kratz, K.; Jung, F.; Lendlein, A.:

Behaviour of fibroblasts on water born acrylonitrile-based copolymers containing different cationic and anionic moieties

In: Clinical Hemorheology and Microcirculation (2012) IOS Press

DOI: 10.3233/CH-2012-1606

Behaviour of fibroblasts on water born acrylonitrile-based copolymers containing different cationic and anionic moieties

N. Scharnagl, B. Hiebl, K. Trescher, M. Zierke, M. Behl, K. Kratz, F. Jung, A. Lendlein*

Center for Biomaterial Development and Berlin Brandenburg Centre for Regenerative Therapies (BCRT), Helmholtz-Zentrum Geesthacht, Kantstr. 55, 14513 Teltow, Germany

ABSTRACT

The chemical composition of a substrate can influence the adhesion, viability and proliferation of cells seeded on the substrate. The aim of this work was to investigate the influence of different cationic or anionic moieties in acrylonitrile based copolymers on the interaction with fibroblasts. A series of ten different types of acrylonitrile based copolymers with a random sequence structure was prepared using a water born synthesis process to exclude potential residues of organic solvents. As charged comonomers cationic methacrylic acid-2-aminoethylester hydrochloride (AEMA), *N*-3-amino-propyl-methacrylamide-hydrochloride (APMA) and anionic 2-methyl-2-propene-1-sulfonic acid sodium salt (NaMAS) were utilized. By application of a specific sintering procedure the copolymer materials were processed into transparent disks for conducting cell tests in direct contact. The copolymers were analyzed with respect to their composition and surface properties.

Cytotoxicity tests of the polymer extracts, as well as of the disks were performed with L929 mouse fibroblasts. All copolymers showed no cytotoxic effects Furthermore for higher molar ratios of AEMA and NaMAS (> 4.4 and 9.9 mol-%) a reduction in cell growth could be observed, which might be a hint that higher charge densities are unfavorable for the proliferation of L929 cells.

Keywords: acrylonitrile, copolymers, fibroblasts, surface charges, biocompatibility

*corresponding author: Prof. Andreas Lendlein, e-Mail: andreas.lendlein@hzg.de

INTRODUCTION

Currently, various polymer-based materials are used in applications involving contact with cells such as cell/tissue-culture systems or implant materials. Materials such as polystyrene (PS), polycarbonate (PC), and polypropylene (PP), are applied as common bulk materials in cell culture [15,19,27]. Copolymers from acrylonitrile (AN) and co-monomers like cationic methacrylic acid-2-aminoethylester hydrochloride (AEMA) or anionic 2-methyl-2-propene-1-sulfonic acid sodium salt (NaMAS) have been explored as a possible substrate for cultivating fibroblasts. The interaction of the copolymers with human skin fibroblasts was investigated considering that these cells are among the first to colonize materials upon implantation or with prolonged external contact [3,29]. For these biomaterials the cell growth correlated with the charge characteristic of the monomer. The adhesion and proliferation of human skin fibroblasts was favored on copolymers containing cationic AEMA, while, in contrast, the presence of NaMAS with anionic groups decreased both the attachment and proliferation of fibroblasts [1,8]. This demonstrates that cellular functions are the result of highly diverse interactions between cells and biomaterials.

However, until now, most biomaterials currently available do not completely meet the complex demands. They are not specifically adapted for applications in contact with cells or other biomedical environments [24]. For commercially available polymers mostly neither biological relevant data nor information on their medical grade purity (chemical purity, cytotoxicity or endotoxin content) are available. The standard production methods for AN-based copolymers are radical polymerizations in *N*,*N*'-dimethylformamide (DMF) or *N*,*N*'-dimethylsulfoxide (DMSO) as solvent [11-13,16-18,20-23,28,31,33,34]. This makes the resulting material potentially toxic for cells as these solvents cannot be removed completely by any drying method or reprecipitation procedure because of the strong intermolecular interaction of the solvent [4-6,14,25,30].

Therefore, a water born suspension polymerization was applied for the synthesis of the AN-based copolymers in technical scale, in which only water, the necessary monomers, and the water soluble initiator were present. Furthermore all cleaning and drying steps were performed in a way, which prevented contamination of the materials. Each processing step of the resulting materials was followed by an extensive characterization by several physico-chemical methods to explore the impact of the processing on the material properties.

With these materials the study aimed to analyse the impact of positive and negative surface charge density on adherence, viability, integrity of the cell membrane, mitochondrial activity, and the morphology of a continuous fibroblast like cell line (L929). Therefore, based on our

medical grade type of synthesis, we produced materials with increasing density of positive or negative charge by increasing the content of the charged comonomer. For acrylonitrile-2-aminoethyl-methacrylate-copolymer (p(AN-*co*-AEMA)) and acrylonitrile-*N*-(3-amino-propyl-methacrylamide)-copolymer (p(AN-*co*-APMA)) the amino content (positively charged by primary amino group) was adjusted by a content of AEMA or APMA of 0.5, 1.0, and 2.0 mol-% in the feed. In case of acrylonitrile-sodium 2-methyl-2-propene-1-sulfonate copolymer (p(AN-*co*-NaMAS)) the negative charge content was increased by the sulfonate content (NaMAS content of the feed 0.5, 1.0 and 2.0 mol-%).

MATERIALS AND METHODS

Material synthesis

The basic AN monomer (Aldrich, > 99% purity) was distilled before use, whereas the other comonomers, AEMA (Aldrich; > 90% purity), APMA (Polyscience, Inc.; 98% purity), and NaMAS (Aldrich; 98% purity) as well as the initiator-system of potassium metabisulfite (KMBS) and potassium persulfate (KPS) were used without further purification. Prior synthesis the chemicals were analysed by Fourier-Transform infrared spectroscopy (FT-IR) and in case of monomers additionally by ^{1}H- and ^{13}C-nuclear magnetic resonance spectroscopy (NMR). All polymers were synthesized in technical scale by solvent free emulsion polymerisation in a batch size of 1 kg. The monomers were dissolved in 8 L of water (Millipore grade) at room temperature in a 20 L double-wall reactor equipped with external cooling. When the reaction was started with the initiator-system KMBS/KPS the temperature inside the reactor increased by about 15 °C. When the temperature decreased to RT again, the reaction was stirred for another 16 h to complete the reaction. Hydrochloric acid (HCl) was added and the precipitated polymer was removed from the reaction mixture by filtration. The product was washed with 40 L of water (Millipore grade) and afterwards dried at 30 °C at 2 mbar until constant weight was achieved. The obtained (co)polymers were characterised by FT-IR, NMR, differential scanning calorimetry (DSC), thermal gravimetric analysis (TGA), gel-permeation chromatography (GPC), headspace gas chromatography (GC-Headspace), and elemental analysis (EA), in which carbon, hydrogen, nitrogen and sulphur (CHNS) were simultaneously detected. The molar composition of the different copolymers was calculated on the basis of the values obtained for the S and N content.

Processing of disk shaped test specimen

For preparation of test specimen with a diameter of 13 mm and a thickness of 1 mm the copolymer was first homogenised by milling, then dried at 60 °C in vacuum and in a next step for each specimen 120 mg of the copolymer were inserted into a custom made tool and sintered under a load of 2000 kg at 120 °C for 30 s and subsequently at 70 °C for 90 s. The disc shaped samples were sterilized with ethylene oxide (45 °C, exposure time: 180 min) prior to surface characterization and biological tests.

Material characterization

Nuclear Magnetic Resonance (NMR)

The composition of the synthesized copolymers, as well as their sequence structure, was analyzed by ^{1}H-NMR spectroscopy using deuterated *N*,*N*'-dimethylsulfoxide or *N*,*N*'-dimethylformamide (DMF) as solvent and tetramethylsilane (TMS) as internal standard recorded on a 500 MHz Avance spectrometer (Bruker, Karlsruhe, Germany). Experiments were performed at ambient temperature with 500 MHz (^{1}H) resonance frequency and a spectral width of 10000 Hz.

Gel Permeation Chromatography (GPC)

The number average molecular weight (M_n) of the synthesized copolymers was analyzed by gel permeation chromatography (GPC). The multidetector GPC consisted of a GRAM VS1 precolumn (40 mm x 4.6 mm), a GRAM 30Å 5091312 and a GRAM 1000Å 71111 column (both 250 mm x 4.6 mm) (all *PSS*, Mainz, Germany), a CO-200 column oven (*W.O. electronics*, Langenzersdorf, Austria), an isocratic pump 980, an automatic injector 851-AS, a LG 980-02 ternary gradient unit, a multiwave length detector MD-910, a RI detector RI-930 (all *Jasco*, Gross-Umstadt, Germany), a differential viscometer η-1001 (WGE Dr. Bures, Dallgow-Doeberitz, Germany), a Wyatt miniDawn Tristar light scattering detector (*Wyatt Technology Corporation*, Santa Barbara, USA), a degasser ERC-3315α (*Ercatech*, Berne, Switzerland). DMF was used as eluent (containing 0.4 wt% toluene as internal standard) at 35 °C with a flow rate of 1.0 mL·min^{-1}. Polystyrene samples were used for universal calibration. Chromatograms were analysed with WINGPC 6.2 (*PSS*) software.

Differential Scanning Calorimetry (DSC)

Differential scanning calorimetry (DSC) was carried out on a Netzsch DSC 204 (Selb, Germany) between –100 °C and 200 °C under nitrogen atmosphere with a constant heating and cooling rate of 20 °C·min^{-1}. The samples were heated from 20 °C to 200 °C, cooled

to -100 °C, and then heated to 200 °C again. The glass transition temperature was determined from the second heating run.

Thermo Gravimetric Analysis (TGA)

Thermal gravimetric analysis (TGA) was carried out on a TG 209C (Netzsch, Selb, Germany) under nitrogen atmosphere between 25 °C and 500 °C with a heating rate of 10 °C·min^{-1}.

Contact Angle (CA) Measurement

The wettability of AN-based copolymers was examined by dynamic contact angle (CA) measurements using captive bubble method at ambient temperature with a DSA 100 (KRÜSS, Hamburg, Germany). The diameter of the contact area between the surface and the bubble was around 2 mm. At least ten measurements on three different locations were performed and averaged to yield the contact angles and their standard deviation.

Profilometry

Surface profiles of the copolymers were obtained with an optical profilometer type MicroProf 200 equipped with a CWL 300 (Fries Research & Technology GmbH) chromatic white-light sensor. Data acquisition was performed with the software AQUIRE (ver. 1.21), while the evaluation was completed with software MARK III (ver. 3.8b). The lateral resolution was 1–2 µm and ca. 5 nm in z-direction. The surface profile and the roughness (*sRa* = roughness mean value and *sRq* = square roughness mean value) were analysed from a field of 4×250 µm. For fast overview additional three scans on each sample were conducted with scanning areas of 50×50 µm^2. The points and lines were 200×200 (4 pt/µm) and the acquisition rate was 300 Hz.

Infrared (IR)-Spectroscopy and –Microscopy

Fourier Transform infrared spectroscopy analyses were carried out on a Bruker Tensor 27 IR-spectrometer (Bruker-Optics, Ettlingen, Germany) equipped with an ATR unit at a resolution of 4 cm^{-1} with at least 64 scans in the frequency range of 300 cm^{-1} and 5000 cm^{-1}.

Sample surfaces were investigated with a HYPERION 2000 infrared microscope (Bruker-Optics) equipped with an ATR objective (magnification 20x) connected to the infrared spectrometer. Analyses were performed in visual-reflectance mode using 32 scans at a resolution of 4 cm^{-1}. A raster size of 13 × 9 measurement points in an area of 350 × 250 µm was used for mapping. This realized a distance between each measurement point of 27 µm in x- and y-direction for a diameter of 20 µm of the imprinted ATR crystal. The obtained spectra were analyzed with the Software OPUS 6.5 (Bruker).

Raman Microscopy

For the shaped materials depth profiling and mapping by Raman spectroscopy was performed for sterilized and non-sterilized samples. A Bruker Senterra dispersive Raman spectrometer equipped with two lasers (785 and 532 nm) and a motorized x-, y-, and z-table was used for these investigations. Using a Raman objective of 50x magnification for the depth-profiling a step size of 0.5 µm and 20 steps (resulting in a depth of 10 µm) was used while for the mappings an area of 350 × 250 µm (13 × 9 measurement points with distance of 27 µm) was selected. The power of the laser was 50 mW for 785 nm wavelength and for 532 nm 5 mW while for both wavelengths the number of scans was 32 and the aperture 50 µm. In all cases the Bruker OPUS 6.5 software was used for evaluation.

Scanning Electron Microscopy (SEM)

All measurements were carried out with a Zeiss Gemini Supra 40 VP instrument equipped with a thermal field emission emitter and an Everhard-Thornley-Detector (secondary electron). The acceleration voltage was 5 kV in all cases. The samples were sputtered with a conductive coating of Pt/Pd 80/20 to prevent electric charging at the sample surface.

High Performance Liquid Chromatography (HPLC)

HPLC measurements were conducted with a Dionex Ultimate 3000 HPLC-System equipped with a Luna-C18 column (Phenomenex), a gradient pump (incl. degasser), and a 4-channel UV/VIS detector. The injection volume was 10 µL. An acetonitrile/water mixture (range from 10/90 to 90/10) was used as eluent at a flow rate of 1 $mL \cdot min^{-1}$ at 20 °C column temperature. Two channels at 195 nm and 210 nm were used for monomer detection. Evaluation of the results was carried out with the Chromeleon®-Software from Dionex.

Gas Chromatography (GC)-Head Space

The content of remaining monomer of the synthesized (co)polymers was analysed on a Hewlett-Packard (series 5890) system, which was equipped with a chromatographic column from Fisons Scientific (type DB624) and a flame ionization detection (FID) unit. The system was calibrated with solutions of acrylonitrile in DMSO in the range between 5 and 100 ppm. The samples were prepared by dissolving 0.5 g of polymer in 4.5 g of DMSO (10% by weight).

Water-/Medium-Uptake Experiments

For water and medium-uptake experiments 0.3 g of dry polymer powder were weighed in adequate sample tubes. 20 mL of water or medium were added and the sealed tube was

shaken for 24 h at 2 Hz at room temperature. Afterwards the polymer powder was filtered through a paper filter and weighed again. When constant weight was achieved after drying in a vacuum oven at 60 °C the mass was determined again. The uptake was then calculated by ratio of the weight of the wet sample divided by weight of the redried sample multiplied with 100.

Analysis of endotoxin content

Prior to cell exposure, copolymer samples were analyzed for their content of endotoxin. Therefore, extracts were obtained and tested with the Limulus Amebocyte Lysate assay (LAL assay; QCL-1000®, Lonza, Cologne, Germany) according to manufacturer instructions.

Culture of L929 cells

According to the international standard EN ISO 10993-5 cytotoxicity tests were performed with cells derived from normal subcutaneous areolar and adipose tissue of a 100-day-old male C3H/An mouse (L929 cells; provided by the American Type Culture Collection, ATCC, Wesel, Germany). For cell expansion continuous subcultures of these cells were maintained under standard environmental conditions (humidified atmosphere, 5 vol-% CO_2 in air, 37 °C; NuAire, Incubator, Germany) on polystyrene using minimal essential medium (MEM Biochrom, Berlin, Germany) supplemented with 10 wt-% horse serum (ATCC, Wesel, Germany) and 1 wt-% penicillin/streptomycin/glutamine (Invitrogen, Darmstadt, Germany). Every second day, the culture medium was changed. The cells were subcultured when they reached a subconfluence of about 80% by rinsing them with phosphate buffered saline, and by subsequent trypsinization using trypsin-EDTA solution (trypsin 0.25 wt-% and ethylene-diaminotetraacetic acid 0.53 mM).

Cytotoxicity Tests

The copolymers were tested for cytotoxic effects using *in vitro* cell tests under static conditions in accordance with the supplier's instructions and in conformity with the EN DIN ISO standard 10993-5. Two test procedures were performed: test of copolymer extracts on L929 cells (indirect test) and, in addition, tests by direct contact of material and L929 cells (direct test).

Sample preparation and the procedure for generating the extract of the materials were performed according to EN ISO 10993 part 12. Copolymer samples were exposed to serum-free cell culture medium (MEM) under permanent stirring at 37 °C for three days. The resulting extract was then used as cell culture medium for L929 cells. L929 cells were seeded on a polystyrene based cell culture 96-multiwell plate (Greiner Bio-One, Solingen, Germany).

After reaching a subconfluent cell layer of about 50%, the culture medium was replaced by the extract. 48 hours later the viability of the cells, integrity of the cell membrane, mitochondrial activity, and cell morphology were analyzed.

For direct testing copolymer discs were inserted in 24-multiwell plates (Greiner Bio-One, Solingen, Germany) and were then seeded with L929 cells. 47,400 cells/cm^2 had to be seeded (according to pre-tests) so that after 48 hours a confluence of ~80% was reached (EN ISO 10993-5). Again the cells viability and morphology were analyzed and LDH and MTS assays were performed.

Cell viability

Cell viability was assessed using fluorescein diacetate (FDA) and propidium iodide (PI) staining. Adherent cells were immersed in 500 µl/well FDA/PI solution made by diluting 5 µl × 5 mg FDA/mL acetone and 2 µl × 1 mg PI/mL PBS in MEM. After 5 min at 37 °C in the dark, cells were subjected to fluorescence microscopy with excitation at 488 nm and detection at 530 nm (FDA), as well as excitation at 543 nm and detection at 620 nm (PI).

Mitochondrial function studies

As many cell processes require the activity of mitochondria, a measurement of the activity of mitochondrial dehydrogenases helps to establish the level of cell activity. The activity of mitochondrial enzymes of the cells was measured by use of a tetrazolium compound 3-(4,5-dimethylthiazol-2-yl)-5-(3-carboxymethoxyphenyl)-2-(4-sulfophenyl)-2H-tetrazolium (MTS), which when reduced produces a colored formazan product (MTS) that is soluble in tissue culture medium (CellTiter® 96 Aqueous Assay, Promega, Germany). The absorbance of the colored formazan product was measured at 492 nm using the SpectraFluor Plus (TECAN, Männedorf, Switzerland) spectrophotometer.

Lactat dehydrogenase (LDH)-release measurement

The activity of the cytoplasmatic enzyme lactate dehydrogenase (LDH) was measured by use of a colorimetric assay in the cell culture supernatant (Cytotoxicity Detection Kit (LDH), Roche, Germany) to evaluate the integrity of the cell plasma membrane at 492 nm using a TECAN SpectraFluor Plus spectrophotometer (TECAN). LDH is located solely within the confines of the cell. The appearance of LDH in the cell culture supernatant therefore indicates that the integrity of the cell membranes has been compromised.

Cell morphology assessment

The morphological phenotype of the cells was evaluated according to the USP 23-NF18 (US Pharmacopeial Convention) and the ISO 10993-5 using a phase contrast microscope in transmission (Zeiss, Jena, Germany) based on the cell shape and the organization of the cell layer. The number of cells on the samples was calculated as mean cell number from five different fields of view.

All experiments were performed in accordance with the ethical guidelines of *Clinical Hemorheology and Microcirculation* [2].

Statistics

Data are given as mean value ± standard deviation for continuous variables and analyzed by a two-sided Student's t-test for paired samples. A p value of less than 0.05 was considered significant.

RESULTS AND DISCUSSION

Material characterization

The acrylonitrile-based homopolymer (PAN) as well as three sets of copolymers, in which the comonomer ratio was varied between 0.5 and 2 mol-% were obtained from the water borne synthesis process (Table 1). The absence of residual monomers of the obtained (co)polymers was proven by IR, TGA, and NMR. In addition, no residual monomers were found by GC-Headspace and HPLC investigations.

The real copolymer compositions were calculated from element composition determined by EA and differed from the nominal molar ratio of the feed concentration due to the different reaction kinetics of the comonomers, which caused a change of the molar ratio during polymerization. This resulted in a non-proportional higher amount of AEMA or APMA in the obtained copolymers, e.g. the AEMA content was higher by a factor of two (2 to 4.4) and in case of APMA by a factor of 5 (2 to 9.9) compared to the feed composition. The yield related to the starting amount of acrylonitrile monomer was higher than 80% (except for p(AN-*co*-AEMA) 4.4) for all copolymerizations. For copolymers with cationic monomers the number averaged molecular weight M_n was in the range of 21 and 31 x 10^{-3} g·mol^{-1} with polydispersities (M_w/M_n) between 2.3 and 3.9 while for anionic systems the molecular weights were in the range between 36 and 51 x 10^{-3} g·mol^{-1} with polydispersities around 4.8. The glass transition temperatures (T_g) of all copolymers determined by DSC were similar to the T_g of polyacrylonitrile homopolymer (see Table 1). As the cell interaction depending on the properties of polymer-based biomaterials can be altered when exposed to a cell-culture

medium, we explored the uptake of water and cell-culture medium without and with horse serum (Figure 1). For all copolymers the uptake of pure water has the highest value (>1500%) followed by serum free cell-culture medium (appr. 1300%) and cell-culture medium including serum (appr. 1100%). This decrease follows the concentration increase of ions and peptides in the used liquids. After drying the mass of the powder increases related to the initial weight of the powder before it was in contact with the liquid because adsorbed residues of ions and peptide remain on the surface of the polymer powder. To investigate whether the media wash out any residue from the copolymer itself, tests were carried out by HPLC. For all polymer systems no residue could be detected.

Table 1: Basic characterization of the resulting copolymers.

Copolymer	Nominal composition (mol-%)	Real composition* (mol-%)	Yield rel. to AN (%)	Molecular Weight M_n (10^3g·mol^{-1})	Poly-dispersity (M_w/M_n)	$T_{g,o}$ [a),**] (°C)	T_g ** (°C)
p(AN-*co*-NaMAS) 0.9	0.5	0.9	92.3	51	4.9	85	100
p(AN-*co*-NaMAS) 1.2	1	1.15	97.1	36	4.7	87	103
p(AN-*co*-NaMAS) 1.5	2	1.47	88.6	46	4.9	87	104
p(AN-*co*-AEMA) 1.4	0.5	1.4	99.5	31	3.6	85	90
p(AN-*co*-AEMA) 1.6	1	1.6	98.5	26	2.3	84	105
p(AN-*co*-AEMA) 4.4	2	4.4	79.3	23	2.4	79	100
p(AN-*co*-APMA) 4.2	0.5	4.2	89.9	31	3.5	86	100
p(AN-*co*-APMA) 4.3	1	4.3	94.3	24	3.3	83	93
p(AN-*co*-APMA) 9.9	2	9.9	83	21	3.9	87	96
PAN	100	100	99	34	5.5	100	102

(a) Onset of T_g; **Calculated by elementary analysis; ** determined by DSC)*

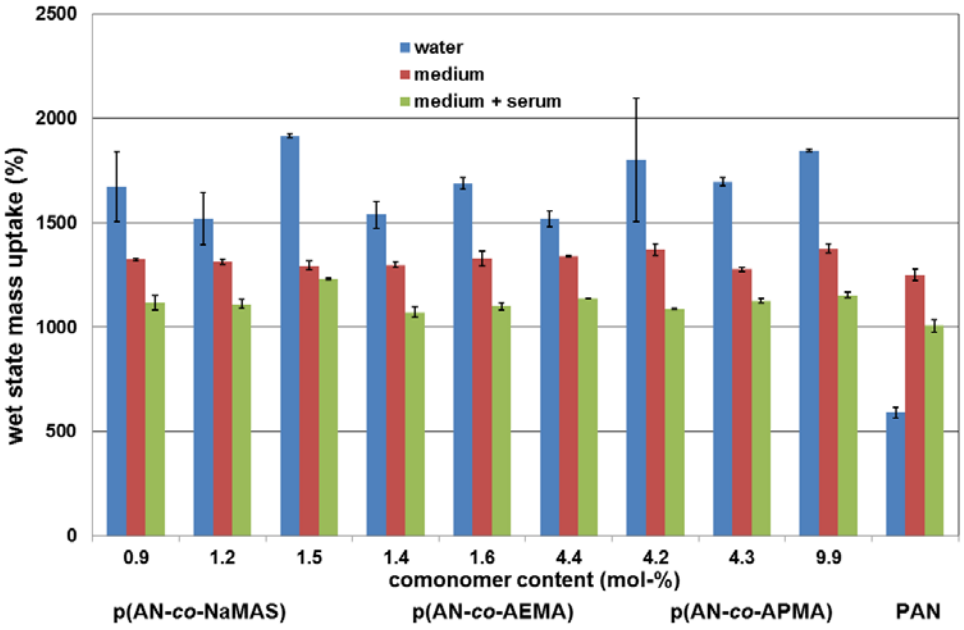

Figure 1: Uptake of water or cell-culture medium (with and without horse serum), n=2-4.

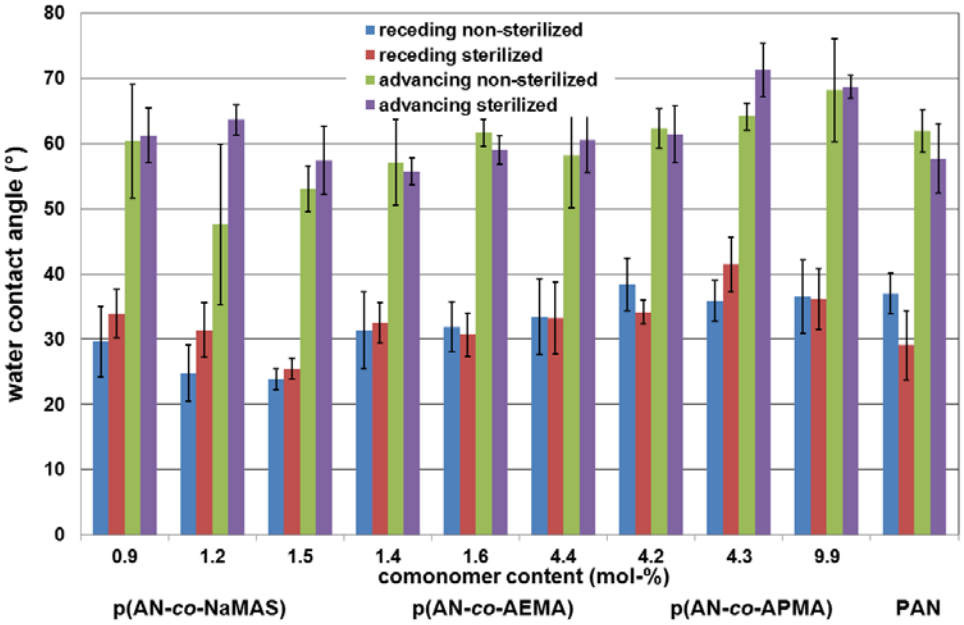

Figure 2: Water contact angles of copolymer disks before and after sterilization (n=5 each).

PAN disks were found to be moderately wettable materials with water contact angles of about 60 ± 9° for the advancing (wetting) and about 35 ± 6° for the receding (dewetting) mode (Figure 2). No significant change of wettability can be observed after sterilization as all values are in the range of the standard deviation. Changes in the hydrophilicity of charged comonomer containing copolymers which could have occurred could not be observed. This indicates that the influence of the formation process on the water contact angles by surface morphology (roughness) might override the changes in wettability caused by the polymer composition. The copolymerization of AN with NaMAS resulted in only minor changes of wettability displayed by a small decrease in the receding water contact angles from 32 ± 4° to 25 ± 2° with increasing NaMAS concentration. The APMA copolymer materials with content higher than 4.3 mol-% have higher advancing contact angle and hence represented a more hydrophobic surface when compared to the pure PAN material (66° to 60°) while the receding contact angle for all copolymers containing cationic comonomers are not different to the PAN homopolymer. This indicates that during exposure to aqueous media a steady state for the contact angel will be reached and the hydrophobicity will not differ.

With Infrared- and Raman-microscopy the surfaces of the polymer disks were investigated to evaluate the chemical homogeneity of the surface (Figure 3 and Figure 4). The characteristic bonds of the different repeating units were identified (e.g. CN for acrylonitrile 2229 cm^{-1}, C=O for AEMA 1713 cm^{-1} or APMA 1710 cm^{-1} and C-C 1648 cm^{-1} for NaMAS) and integrated. The resulting mapping of the surface shows only some differences in intensity of the specific bond, which belong to irregularities in thickness of the specimen caused by

unevenness of the formation tool. This was evaluated by comparison of visual microscopy pictures with the corresponding IR- or Raman-mapping (Figure 3 and Figure 4).

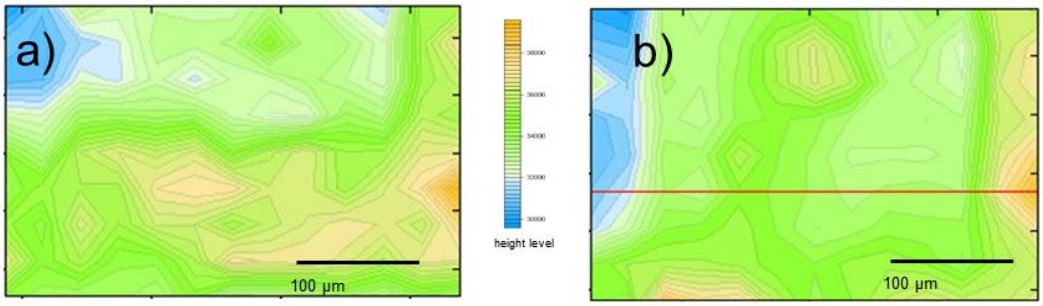

Figure 3: Exemplary IR Mappings of a) p(AN-*co*-NaMAS) 1.5 and b) p(AN-*co*-AEMA) 1.6 disks after sterilization (Integration of CN-bond corresponding to AN); bar: 100 µm.

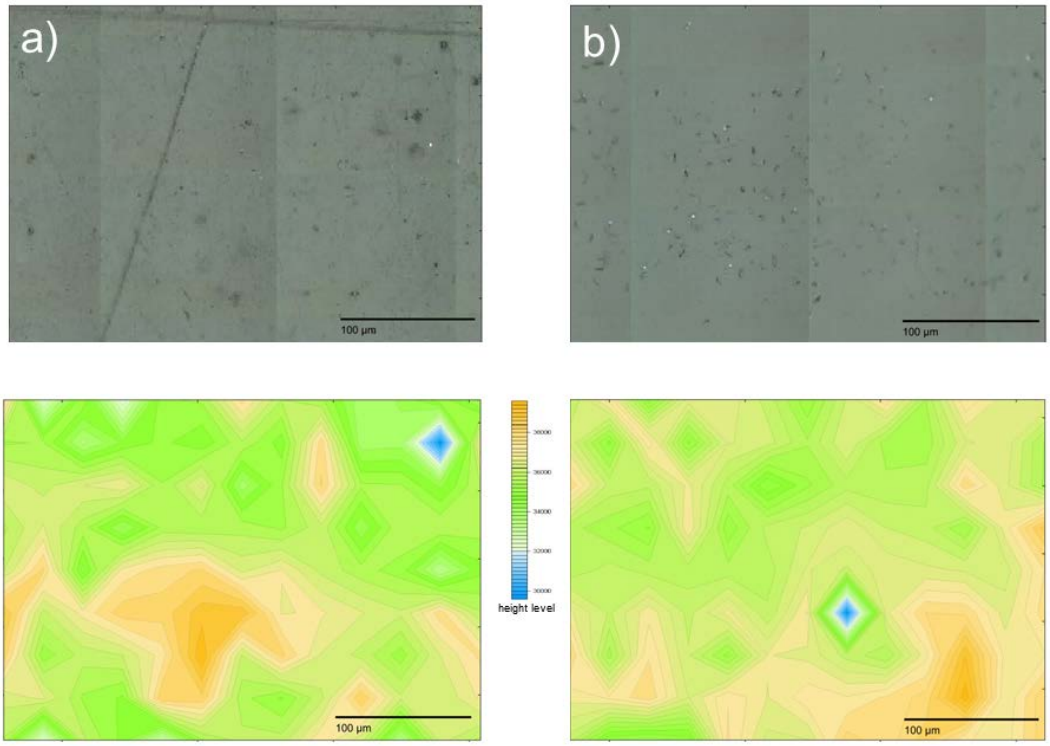

Figure 4: Exemplary mappings of a) p(AN-*co*-NaMAS) 1.5 und b) p(AN-*co*-AEMA) 4.4 disk after sterilization. Upper pictures: VIS-mapping. Lower pictures: Raman-mapping of integrated CN-bond corresponding to AN; bar: 100 µm.

In addition to the surface chemistry also the morphology of the surfaces plays an important role for the proliferation and adhesion of cells on polymer-based materials [24]. Therefore the surface topology was investigated by SEM and profilometry. Figure 5 is showing that the surface planarity is a critical issue. Every scratch, damage or failure of the formation tool is replicated on the surface of the test specimen as shown in Figure 6 and Figure 7 exemplarily for profilometry and SEM images. Therefore the standard deviation and error bars of the roughness data are relatively large (up to 50%). With respect to these circumstances no significant difference in roughness of the materials can be reported and therefore cannot be

taken into account for a discussion on influencing the cell behaviour during the exposure to L929 fibroblasts.

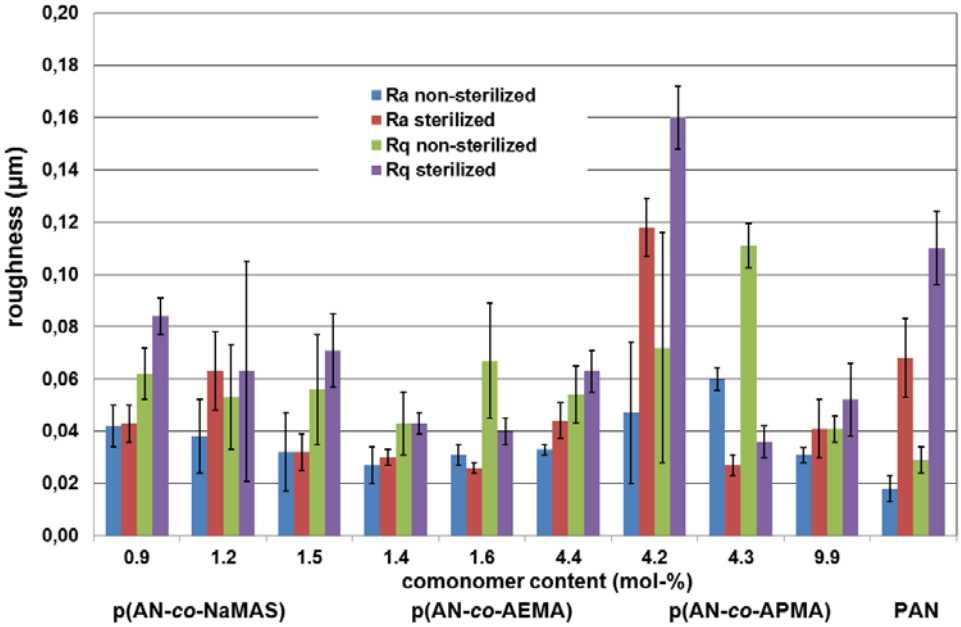

Figure 5: Roughness of sterilized and non-sterilized specimen; n = 3 or 6; R_a = roughness mean value and R_q = square roughness mean value.

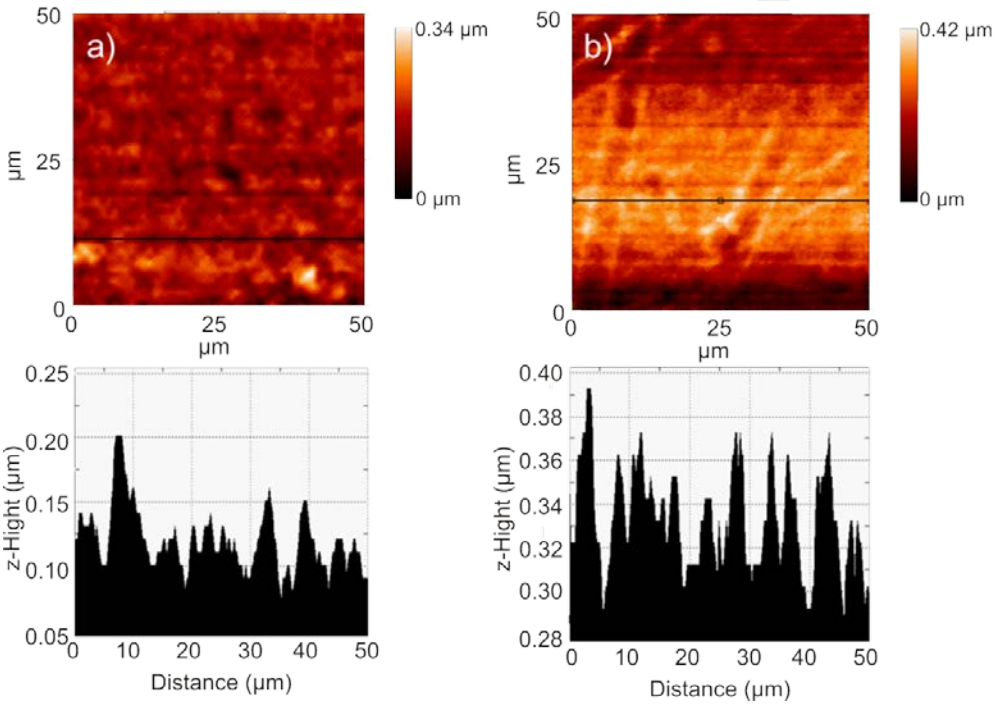

Figure 6: Profilometry data of a) p(AN-*co*-NaMAS) 1.5 and b) p(AN-*co*-AEMA) 4.4 disks after sterilization. Upper part: mapping of 50 x 50 µm area. Lower part: profile diagram of the mapping at the black line.

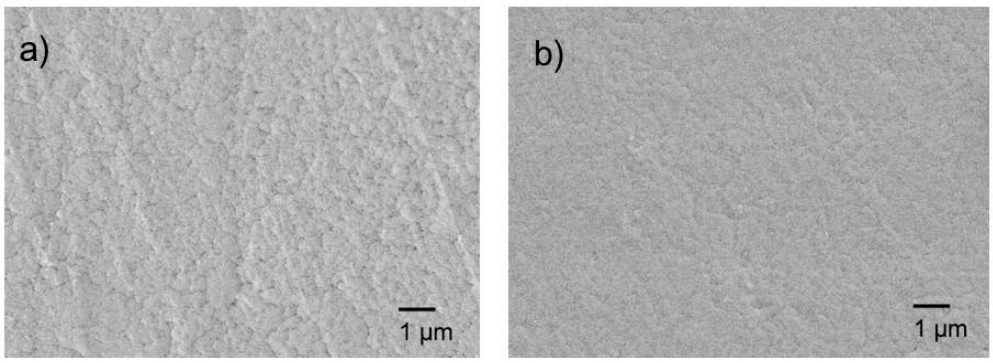

Figure 7: Exemplary SEM photographs of disks of a) p(AN-*co*-NaMAS) 1.5 and b) p(AN-*co*-AEMA) 4.4 after sterilization; bar: 1 µm.

Endotoxin content

Endotoxin values below 0.06 EU/ml were detected for all copolymer samples. According to the US Food and Drug Administration, this is below the limit for biomaterials of 0.5 EU/ml [7].

Cytotoxicity testing

Indirect tests showed that there were no or only slight influences on the integrity of the cell membranes or on the mitochondrial activity of the L929 cells 48 h after being cultured in the copolymer extracts. In addition, the morphology of the L929 cells was not different to the morphology of these cells 48 h after culturing them with pure cell culture medium (control).

Cell viability and function

Additionally, direct cell tests were performed. The cytotoxicity of the substrates (sintered discs of p(AN-*co*-AEMA) 1.4, p(AN-*co*-AEMA) 1.6 , p(AN-*co*-AEMA) 4.4, p(AN-*co*-APMA) 4.2, p(AN-*co*-APMA) 4.3, p(AN-*co*-APMA) 9.9, p(AN-*co*-NaMAS) 0.9, p(AN-*co*-NaMAS) 1.2, and p(AN-*co*-NaMAS) 1.5) was analyzed *in vitro* using fibroblast cells (L929) cultured for 48 hours at 37 °C. Staining - using fluorescein diacetate (FDA) and propidium iodide (PI) - indicated that almost 100% of the adherent cells on p(AN-*co*-AEMA), p(AN-*co*-APMA), p(AN-*co*-NaMAS) and PAN were viable 48 h after seeding.

The activity of intracellular dehydrogenases on glass (control), p(AN-*co*-AEMA), p(AN-*co*-APMA), p(AN-*co*-NaMAS) and PAN was not influenced by the increased concentrations of AEMA, APMA or NaMAS (Figure 8; $n = 8$ each, $p > 0.05$ each), suggesting that the mitochondrial activity was not negatively affected by the different polymers.

LDH release

There were no or only slight differences in the cellular LDH-release on the different substrates related to the concentrations of AEMA, APMA or NaMAS 48 h after seeding

(Figure 9), indicating that the integrity of the cell membranes remained unchanged (n = 8, p > 0.05 each)

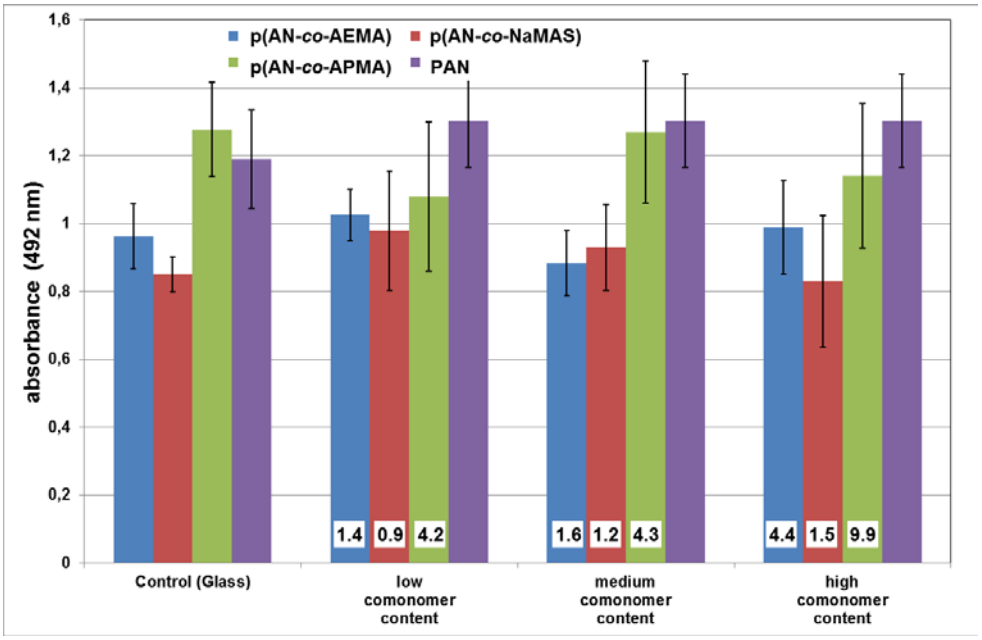

Figure 8: Activity of mitochondrial enzymes of L929 cells on polyacrylonitrile (PAN) copolymerized with different comonomer content of AEMA, APMA and NaMAS (the comonomer content in mol-% is represented by the numbers in the bars), measured by a MTS assay; glass was used as control; CellTiter® 96 Aqueous Assay, Promega, Germany; means ± standard deviation, n = 8 each.

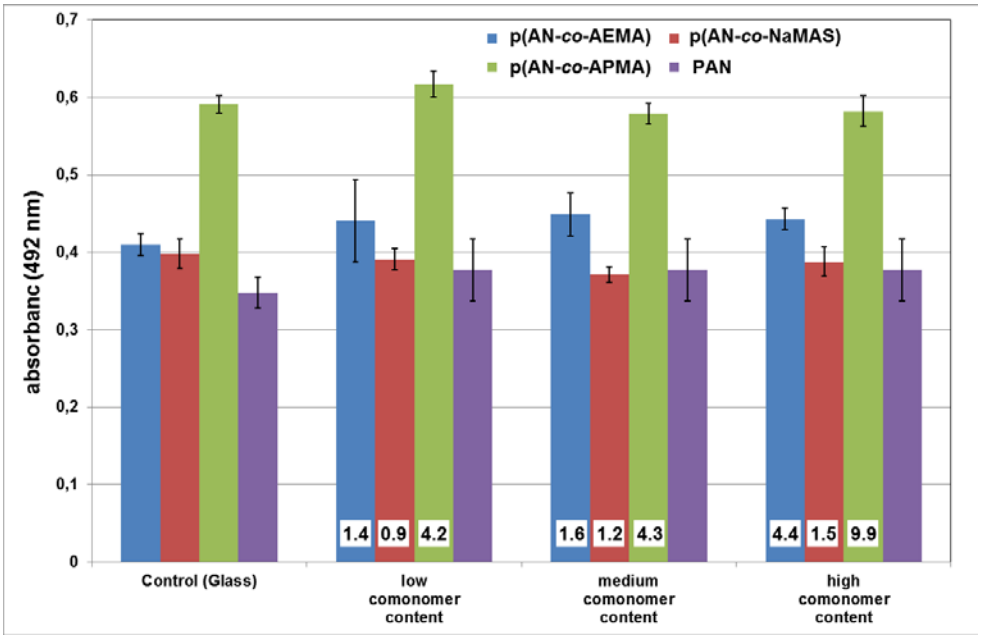

Figure 9: LDH release 48 h after growing L929 cells on the homopolymer PAN as well as copolymerized with different comonomer content of AEMA, APMA and NaMAS (the comonomer content in mol-% is represented by the numbers in the bars); glass was used as control, LDH assay (Roche, Germany); means ± standard deviation, n = 8 each.

Cell morphology and cell density

Figure 10 shows the typically morphologies of L929 cells cultured for 48 hours on the different copolymers and controls (glass), respectively. The morphological phenotype of the cells changed from spindle shaped and weakly sprouted to more flattened and more sprouted types, which can be attributed to the (slightly) increasing AEMA-, APMA- and NaMAS-content. In general, the number of adherent cells was higher on glass (713 ± 23 cells/mm^2) than on the acrylonitrile-based copolymers 48 h after seeding, reaching almost confluence 48 h after seeding. Cells, which underwent mitosis were much more frequent on glass than on p(AN-*co*-AEMA), p(AN-*co*-APMA) or p(AN-*co*-NaMAS).

On p(AN-*co*-AEMA) the confluence was between 60% and 80%; the number of adherent cells increased significantly ($p < 0.05$) with increasing AEMA content (p(AN-*co*-AEMA) 1.4: 294 ± 17 cells/mm^2, p(AN-*co*-AEMA) 1.6: 430 ± 27 cells/mm^2, p(AN-*co*-AEMA) 4.4: 486 ± 17 cells/mm^2). On the p(AN-*co*-AEMA) 4.4 cell morphology was comparable to that of cells grown on glass (control).

The confluence of the cells on p(AN-*co*-NaMAS) was between 40% and 70%. The numbers of adherent cells on p(AN-*co*-NaMAS) 0.9, 1.2, and 1.5 did not differ (approximately 500 ± 18 cells/mm^2; $p > 0.05$), but an increasing number of cells was rounded and loosely attached (up to 40% for the NaMAS 1.5).

The confluence of the L929 cells on p(AN-*co*-APMA) was between 50 – 70%. The numbers of adherent cells on p(AN-*co*-APMA) 4.2, 4.3, and 9.9 did not differ (approximately 490 ± 20 cells/mm^2; $p > 0.05$), but an increasing number of cells were rounded and loosely attached (up to 40% for APMA 9.9) while some of the cells showed blebs.

Figure 11 shows L929 cells on the homopolymer PAN. As described earlier the compatibility of PAN is not comparable to that of the copolymers [10,32]. More than 70% of the L929 cells on PAN were rounded and only loosely attached. The cells were viable (the release of LDH as well as the mitochondrial activity of the L929 cells on PAN were not increased compared to controls) but obviously were not able to adhere to the PAN surface with its typical adherent polygonal phenotype. Also a lot of cells blebbed, presented vacuoles, an uneven cytoplasm and granular material appeared in the cytoplasm.

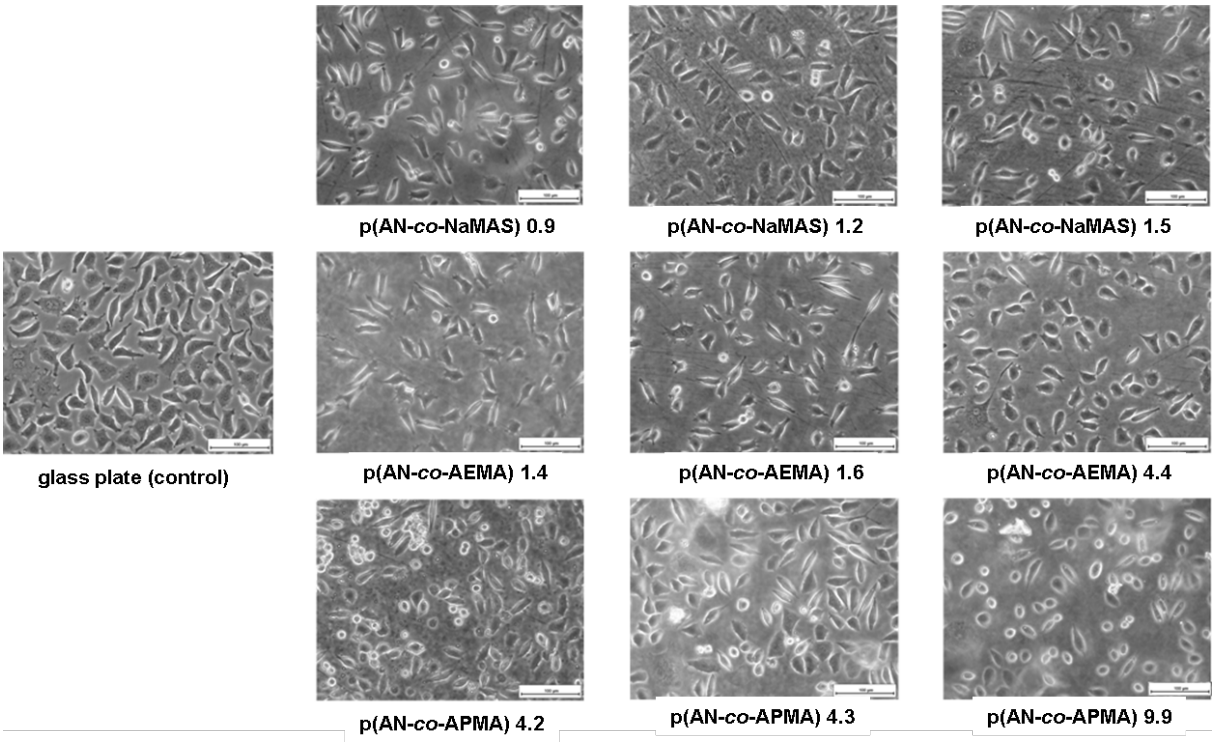

Figure 10: Morphology of L929 cells 48 h after seeding on PAN copolymerized with different amounts of AEMA, APMA and NaMAS (each 0.5, 1.0 and 2.0 mol-% comonomer feed content); glass was used as control (phase contrast microscopy in transmission, primary magnification 1:20).

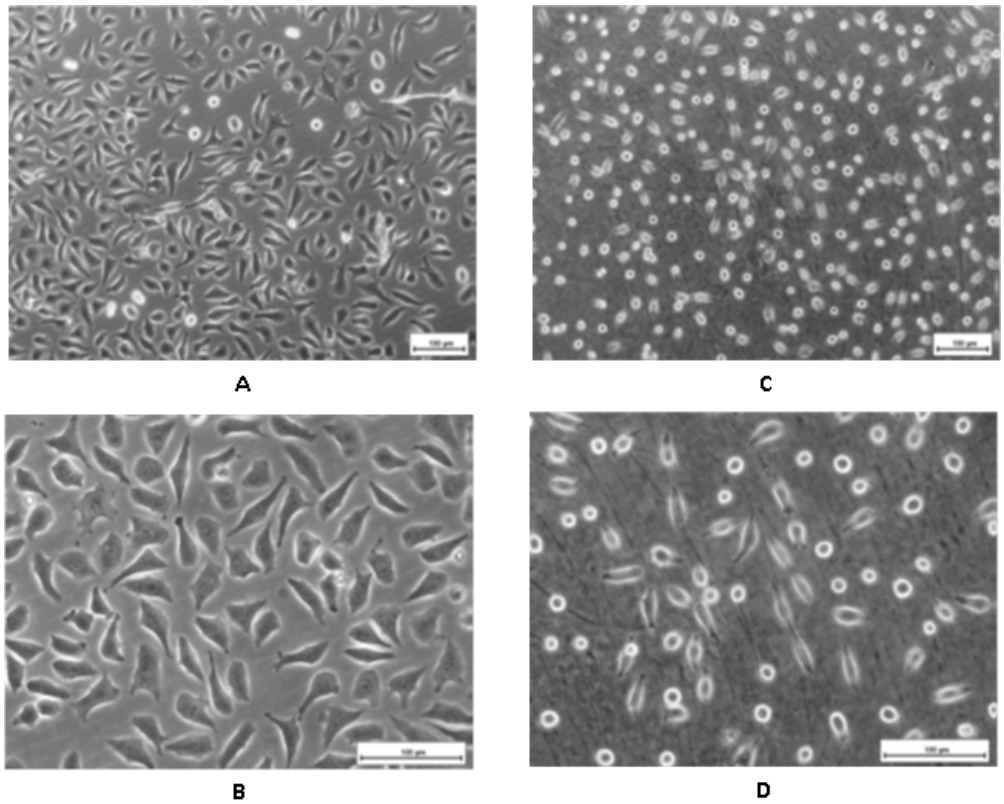

Figure 11: L929 cells on polystyrene (A, B; control) and PAN (C, D) 48 h after seeding (phase contrast microscopy in transmission, primary magnification 1:10 (A, C) and 1:20 (B, D).

CONCLUSION

The study revealed that AN-based copolymers with different types of charges and charge density can be synthesised in technical scale and in medical grade quality. For the copolymer powders no significant differences for the uptake behaviour of water, pure cell-culture medium or cell-culture medium in combination with serum could be detected.

The formation process led to transparent and uniform disks with a homogenous surface chemistry and a comparable hydrophilic surface for all comonomers. Physico-chemical investigations of the shaped polymers before and after sterilization using ethylene oxide did not show any significant differences that could lead to distinct behaviour for the adherence of L929 mouse fibroblasts on the material. However, the formation process still had some technical limits with regard to the surface morphology that resulted in minor irregularities on the evenness. Nevertheless, statistically the surfaces were equal for all specimens that were exposed to L929 fibroblasts.

Cytotoxicity tests with L929 fibroblasts indicated that almost 100% of the adherent cells on p(AN-*co*-AEMA), p(AN-*co*-APMA), p(AN-*co*-NaMAS) and PAN were viable 48 h after seeding. MTS release suggested that the mitochondrial activity was not negatively affected by the different polymers. There were no or only slight differences in the cellular LDH-release on the different substrates related to the concentrations of AEMA, APMA or NaMAS 48 h after seeding, indicating that the integrity of the cell membranes remained unchanged [9].

With increasing comonomer content the morphological phenotype of the cells changed from spindle shaped and weakly sprouted to more flattened and more sprouted types. On p(AN-*co*-AEMA) with increasing content of AEMA the number of adherent cells increased too (294 ± 17 to 486 ± 17 cells/mm^2) and the cell morphology became comparable to that on glass (controls to assure the physiological status of the cells used [26]). For p(AN-*co*-APMA) and p(AN-*co*-NaMAS) the number of adherent cells did not significantly change with increasing content of APMA or a small increase of NaMAS content. Cells became less adherent for APMA 4.2 and NaMAS 0.9 in the copolymer. For the homopolymer PAN the cells were not able to adhere to the surface. The experiments demonstrated that charged AN-based copolymers influence the cell morphology as well as the cell proliferation in case of L929 fibroblasts compared to the homopolymer PAN. Further studies with another series of positively or negatively charged comonomers with a wider range of concentrations should be carried out to evaluate these results. However, these promising results might enable in future cell culture devices in which one cell type of a mixture will grow preferentially or medical devices which favour the growth of a certain cell type and in this way assist autoregeneration.

Acknowledgement

The authors thank Isabelle Sebastien, Daniela Radzik, Elisabeth Luka, Susanne Reinhold, Ruth Hesse, Manuela Keller, Yvonne Pieper, Susanne Schwanz, Robert Jeziorski, Matthias Kahl, Hans-Jörg Ziegler, and Michael Schossig for their technical assistance.

REFERENCES

[1] G. Altankov, W. Albrecht, K. Richau, T.H. Groth and A. Lendlein, On the tissue compatibility of poly(ether imide) membranes: an in vitro study on their interaction with human dermal fibroblasts and keratinocytes, *Journal of Biomaterials Science-Polymer Edition* **16** (2005), 23-42.

[2] Anonymous, Ethical guidelines for publication in Clinical Hemorheology and Microcirculation, *Clin Hemorheol Microcirc* **44** (2010), 1-2.

[3] G. Boese, C. Trimpert, W. Albrecht, G. Malsch, T. Groth and A. Lendlein, Membranes from acrylonitrile-based polymers for selective cultivation of human keratinocytes, *Tissue Engineering* **13** (2007), 2995-3002.

[4] C. Capo, Z. Mishal, V. Balloy, A.M. Benoliel and P. Bongrand, Dimethylsulphoxide induction of the murine macrophage-like line P388D1: change of phagocytic ability and cell surface properties, *J Cell Sci* **64** (1983), 281-93.

[5] T.G. Christensen, B. Burke, D.L. Dexter and N. Zamcheck, Ultrastructural Evidence of Dimethylformamide-Induced Differentiation of Cultured Human-Colon Carcinoma-Cells - Increased Expression of Desmosomes, *Cancer* **56** (1985), 1559-1565.

[6] M. Fiore and F. Degrassi, Dimethyl sulfoxide restores contact inhibition-induced growth arrest and inhibits cell density-dependent apoptosis in hamster cells, *Experimental Cell Research* **251** (1999), 102-110.

[7] M.B. Gorbet and M.V. Sefton, Endotoxin: the uninvited guest, *Biomaterials* **26** (2005), 6811-7.

[8] T. Groth, B. Seifert, G. Malsch, W. Albrecht, D. Paul, A. Kostadinova, N. Krasteva and G. Altankov, Interaction of human skin fibroblasts with moderate wettable polyacrylonitrile-copolymer membranes, *Journal of Biomedical Materials Research* **61** (2002), 290-300.

[9] B. Hiebl, K. Lutzow, M. Lange, F. Jung, B. Seifert, F. Klein, T. Weigel, K. Kratz and A. Lendlein, Cytocompatibility testing of cell culture modules fabricated from specific candidate biomaterials using injection molding, *Journal of Biotechnology* **148** (2010), 76-82.

[10] X.J. Huang, Z.K. Xu, L.S. Wan, Z.G. Wang and J.L. Wang, Novel acrylonitrile-based copolymers containing phospholipid moieties: Synthesis and characterization, *Macromolecular Bioscience* **5** (2005), 322-330.

[11] A. Hunyar, H. Reichert, H. Park and M. Kubanczyk, *Continuous production of polyacrylonitrile and its copolymers in dimethylformamide*, Deutsche Akademie der Wissenschaften zu Berlin . 1964, pp. 5 pp.

[12] S.V. Konyukhova, T.F. Sutyagina and O.A. Yakovleva, *Method for manufacturing fabric nonwoven filters useful in production of polyacrylonitrile fibers*, OAO "Nauchno-Issled. Inst. Netkanykh Materialov", 2008, pp. 4pp.

[13] N. Krasteva, B. Seifert, M. Hopp, G. Malsch, W. Albrecht, G. Altankov and T. Groth, Membranes for biohybrid liver support: the behaviour of C3A hepatoblastoma cells is

dependent on the composition of acrylonitrile copolymers, *J Biomater Sci Polym Ed* **16** (2005), 1-22.
[14] M.G. Lampugnani, M. Pedenovi, A. Niewiarowski, B. Casali, M.B. Donati, G.C. Corbascio and P.C. Marchisio, Effects of Dimethylsulfoxide (Dmso) on Microfilament Organization, Cellular Adhesion, and Growth of Cultured Mouse B-16 Melanoma-Cells, *Experimental Cell Research* **172** (1987), 385-396.
[15] J.H. Lee, S.J. Lee, G. Khang and H.B. Lee, Interaction of fibroblasts on polycarbonate membrane surfaces with different micropore sizes and hydrophilicity, *Journal of Biomaterials Science-Polymer Edition* **10** (1999), 283-294.
[16] G. Malsch, J. Barton, V. Horanska-Vaskova and P. Fritzsche, Radical reactions initiated by chelate complexes of transition metals. XV. Synthesis of acrylonitrile-styrene block copolymers, *Acta Polymerica* **31** (1980), 118-23.
[17] G. Malsch, H. Dautzenberg, W. Krippner, D. Scheller, P. Fritzsche and W. Berger, Contributions to the Anionic-Initiated Polymerization of Acrylonitrile .2. The Formation of Branching in Polyacrylonitrile Polymerized in a Flow Tube, *Acta Polymerica* **33** (1982), 626-631.
[18] G. Malsch, P. Fritzsche and H. Dautzenberg, Contributions to the Anionic-Initiated Polymerization of Acrylonitrile .1. Investigation of Branching Reactions, *Acta Polymerica* **32** (1981), 758-763.
[19] H. Matsuyama, T. Maki, M. Teramoto and K. Asano, Effect of polypropylene molecular weight on porous membrane formation by thermally induced phase separation, *Journal of Membrane Science* **204** (2002), 323-328.
[20] M. Okubo, S. Fujii, H. Maenaka and H. Minami, Production of polyacrylonitrile particles by precipitation polymerization in supercritical carbon dioxide, *Colloid and Polymer Science* **281** (2003), 964-972.
[21] A.B. Pakshver, Production of polyacrylonitrile fibers, *Khim. Volokna* (1967), 54-9.
[22] B. Qian, Present situation and developmental trend of polyacrylonitrile fiber industry, *Shanghai Huagong* **29** (2004), 47-49, 53.
[23] J.B. Quig, "Orlon" acrylic fiber-a new synthetic, *Can. Text. J. (1907-1998)* **66** (1949), 42-4,46-7.
[24] N. Scharnagl, S. Lee, B. Hiebl, A. Sisson and A. Lendlein, Design principles for polymers as substratum for adherent cells, *J Mater Chem* **20** (2010), 8789-8802.
[25] F. Sjogren and C. Anderson, The spectrum of inflammatory cell response to dimethyl sulfoxide, *Contact Dermatitis* **42** (2000), 216-221.
[26] Y. Song, J. Feijen, D.W. Grijpma and A.A. Poot, Tissue engineering of small-diameter vascular grafts: a literature review, *Clin Hemorheol Microcirc* **49** (2012), 357-74.
[27] J.G. Steele, C. Mcfarland, B.A. Dalton, G. Johnson, M.D.M. Evans, C.R. Howlett and P.A. Underwood, Attachment of Human Bone-Cells to Tissue-Culture Polystyrene and to Unmodified Polystyrene - the Effect of Surface-Chemistry Upon Initial Cell Attachment, *Journal of Biomaterials Science-Polymer Edition* **5** (1993), 245-257.
[28] J. Szafko and B. Pabin-Szafko, Thermal decomposition of 2,2 '-azoisobutyronitirle. The rate of initiation in the polymerisation of acrylonitrile in N,N-dimethylformamide, *Fibres & Textiles in Eastern Europe* **10** (2002), 66-70.
[29] Y. Tamada and Y. Ikada, Fibroblast Growth on Polymer Surfaces and Biosynthesis of Collagen, *Journal of Biomedical Materials Research* **28** (1994), 783-789.
[30] M.C. Tanzi, P. Verderio, M.G. Lampugnani, M. Resnati, E. Dejana and E. Sturani, Cytotoxicity of Some Catalysts Commonly Used in the Synthesis of Copolymers for Biomedical Use, *Journal of Materials Science-Materials in Medicine* **5** (1994), 393-396.
[31] V.L. Tsiperman, A.B. Pakshver and E.A. Pakshver, *Selection of solvents for production of polyacrylonitrile fibers*, 1966, pp. 158-66.

[32] L.S. Wan, Z.K. Xu, X.J. Huang, Z.G. Wang and P. Ye, Hemocompatibility of poly(acrylonitrile-co-N-vinyl2-pyrrolidone)s: Swelling behavior and water states, *Macromolecular Bioscience* **5** (2005), 229-236.
[33] X. Wang, X. Shen, Q. Feng and F. Cui, *Production of polyacrylonitrile-based hollow fiber carbon membrane for oxygenation units*, Tsinghua University, 2003, pp. 7 pp.
[34] M. Yoshida and M. Taniyama, Production of polyacrylonitrile fibers by slurry-type dissolution in zinc chloride-sodium chloride mixed aqueous solutions. I. Solubility of copolymers, *Sen'i Gakkaishi* **18** (1962), 903-9.